Published in final edited form as:
Gastroenterology. 2008 October ; 135(4): 1288–1300. doi:10.1053/j.gastro.2008.06.089.

Stabilization of β-catenin induces pancreas tumor formation

Patrick W. Heiser[1], **David A. Cano**[1], **Limor Landsman**[1], **Grace E. Kim**[2], **James G. Kench**[3,4], **David S. Klimstra**[5], **Maketo M. Taketo**[6], **Andrew V. Biankin**[3,7], and **Matthias Hebrok**[1,*]

1*Diabetes Center, University of California, San Francisco, CA 94143, USA*

2*Department of Pathology, University of California, San Francisco, CA 94143, USA*

3*Cancer Research Program, Garvan Institute of Medical Research, Sydney, New South Wales, 2010 Australia*

4*Department of Tissue Pathology, Institute of Clinical Pathology and Medical Research, Westmead Hospital, Westmead, New South Wales, 2145 Australia*

5*Department of Pathology, Memorial Sloan Kettering Cancer Center, New York, NY 10021 USA*

6*Department of Pharmacology, Graduate School of Medicine, Kyoto University, Kyoto, Japan 606-8501*

7*Department of Surgery, Bankstown Hospital, Sydney, New South Wales, 2010 Australia*

Abstract

Background & Aims—β-catenin signaling within the canonical Wnt pathway is essential for pancreas development. However, the pathway is normally down-regulated in the adult organ. Increased cytoplasmic and nuclear localization of β-catenin can be detected in nearly all human solid pseudopapillary neoplasms (SPN), a rare tumor with low malignant potential. Conversely, pancreatic ductal adenocarcinoma (PDA) accounts for the majority of pancreatic tumors and is one of the leading causes of cancer death. While activating mutations within β-catenin and other members of the canonical Wnt pathway are rare, recent reports have implicated Wnt signaling in the development and progression of human PDA. Here, we sought to address the role of β-catenin signaling in pancreas tumorigenesis.

Methods—Using Cre/lox technology, we conditionally activated β-catenin in a subset of murine pancreatic cells, *in vivo*.

Results—Activation of β-catenin results in the formation of large pancreatic tumors at a high frequency in adult mice. These tumors resemble human SPN based upon morphological and immunohistochemical comparisons. Interestingly, stabilization of β-catenin blocks the formation of pancreatic intraepithlelial neoplasia (PanIN) in the presence of an activating mutation in Kras that is known to predispose individuals to pancreatic ductal adenocarcinoma (PDA). Instead, mice in which β-catenin and Kras are concurrently activated develop distinct ductal neoplasms that do not resemble PanIN lesions.

Conclusions—These results demonstrate that activation of β-catenin is sufficient to induce pancreas tumorigenesis. Moreover, they indicate that the sequence in which oncogenic mutations are acquired has profound consequences on the phenotype of the resulting tumor.

*__Correspondence__: mhebrok@diabetes.ucsf.edu; Phone: (415) 514-0820; Fax: (415) 564-5813, 513 Parnassus Ave. HSW 1112, Box 0540 San Francisco, CA 94143.

Conflict of interest: None of the authors listed above have a conflict of interest in the work presented in this manuscript.

Keywords

Wnt; β-catenin; pancreas; cancer; SPN; PDA

β-catenin plays two divergent, yet critical, cellular roles. The first is at the plasma membrane, where it interacts with cadherins to form adherins junctions that are important for cell-cell adhesion. The second is at the center of the canonical Wnt signaling pathway, a signaling cascade that is essential for embryonic development and whose disregulation has been implicated in a number of human cancers [1–3]. In the absence of Wnt ligand, β-catenin is targeted for degradation by phosphorylation via its interaction with a complex containing Axin and APC. However, upon binding of Wnt ligand, this complex is inhibited, unphosphorylated β-catenin accumulates in the cytoplasm, and this protein isoform eventually enters the nucleus. After nuclear entry, this stabilized, or "activated", form of β-catenin binds Tcf/Lef transcriptional coactivators resulting in upregulation of Wnt-responsive target genes (reviewed in [4, 5]).

Several recent studies have demonstrated that the canonical Wnt signaling pathway is dynamically regulated during pancreatic development, and that β-catenin, in particular, is essential for normal pancreatic organogenesis [6–10]. However, this pathway is normally downregulated within the adult pancreas [6, 7].

Mutations in β-catenin/APC and/or evidence of aberrant canonical Wnt signaling pathway activity have been found in pancreatoblastomas [11], acinar cell carcinoma [12], pancreatic ductal adenocarcinoma (PDA) [13–15], and solid pseudopapillary neoplasm (SPN) [16–19]. However, a direct causal relationship between Wnt pathway deregulation and tumor development has not been clearly demonstrated in any of these tumor types.

Here, we demonstrate that stabilization of β-catenin within the pancreatic epithelium, including duct cells, results in the formation of tumors that resemble human SPN. Surprisingly, concurrent activation of β–catenin and Kras, a mediator of PDA formation, prevents the formation of pancreatic intraepithelial neoplasias (PanINs) and PDA. Thus, our data present *in vivo* evidence that increased Wnt signaling is sufficient to induce pancreatic tumor formation and that the sequence of oncogene activation is critically important for the formation of different types of tumors.

Materials and Methods

Mice

Noon of the day when vaginal plugs are detected is treated as e0.5 day post coitum. The following mouse lines were used: *β-cat*^{active,} carrying the floxed exon 3 allele of β-catenin [20], Kras^{G12D} mice, carrying a targeted mutation in the first exon of the Kras allele[21], and the *R26R* [22] and *Z/AP* [23] reporter lines. All lines require Cre-mediated recombination for transgene expression and were crossed with strains expressing Cre-recombinase under the control of the endogenous *Ptf1a* promoter[24] or the Pdx1 promoter (*Pdx-Cre*^{early}) [25] and maintained in a mixed background. All transgenic mice used carry a single copy of the indicated transgene.

Tissue preparation, immunohistochemistry, and microscopy

Embryonic tissues were fixed and paraffin wax imbedded as previously described [26]. Adult murine pancreas and tumor tissue was fixed overnight at 4°C in 1x zinc buffered formalin (Anatech, Ltd.). Hematoxylin/eosin staining, immunohistochemical and immunofluorescence analysis were performed as previously described [27] on 6μm sections.

Staining for β-galactosidase activity in whole e11.5 embryos was performed as previously described [28]. Alkaline phosphatase and alcian blue staining methods, antibodies used, morphometric quantitation protocols, quantitative PCR conditions, primer sequences, and western blotting conditions are provided in the Supplemental Methods section.

Results

Ptf1a-Cre mice target a subset of early pancreatic progenitor cells and pancreatic ducts

Previously, we demonstrated that stabilization of β-catenin within most cells of the early pancreatic epithelium using the *Pdx-Cre^{early}* mouse severely disrupts pancreas development leading to neonatal lethality. In contrast, delayed expression of *β-cat^{active}* under the control of a different *Pdx1*-promoter (*Pdx-Cre^{late}*) mainly targets acinar, but not ductal cells. In this context, activation of β-catenin results in a significant increase in acinar cell number without evidence of cellular transformation[28]. To test whether the *Ptf1a* promoter, another pancreatic transcription factor, would allow stabilization of β-catenin within a subset of early pancreatic epithelial cells that include duct progenitors, we directly compared the pattern of Cre-recombinase activity in *Pdx-Cre^{early}* and *Ptf1a-Cre* mice. For this purpose, we used two reporter strains, *R26R*[22] and *Z/AP*[23], which express β-galactisodase or alkaline phosphatase, respectively, upon Cre-mediated recombination.

We found that, like the *Pdx-Cre^{early}* mouse strain (Fig. 1A), the *Ptf1a-Cre* strain has detectable Cre recombinase activity resulting in β-galactosidase staining at e11.5 (Fig. 1C), a time point when ductal progenitors are still being specified [25]. However, while the *Pdx-Cre^{early}* mouse has robust Cre-recombinase activity in the majority of cells within the pancreatic epithelium (Fig. 1B), only a subset of epithelial cells are targeted by the *Ptf1a-Cre* strain (Fig. 1D, black arrows) at this time point. These results are consistent with previous reports [24].

By four weeks of age, the majority of acinar cells within both the *Pdx-Cre^{early}* and *Ptf1a-Cre; Z/AP* mice are positive for alkaline phosphatase (Fig 1E). In addition, pancreatic ducts contain cells that have alkaline phosphatase activity in those mice (Fig 1E, yellow arrows). A subset of pancreatic ducts in the *Ptf1a-Cre; Z/AP* mouse do not show evidence of Cre-recombinase activity and are not positive for alkaline phosphatase (Fig1E, red arrow). Sections from control animals did not exhibit detectable alkaline phosphatase activity within the acinar or ductal compartments (Fig. 1E). Thus, the limited Cre-expression domain within the early pancreas, when β-catenin stabilization is likely to disrupt organogenesis, coupled with effective targeting of pancreatic ductal cells make this mouse line well suited to probe the effects of β-catenin stabilization in adult mice.

Activation of β-catenin in Ptf1a-Cre; β-cat^{active} mice causes ductal lesions and increased pancreas mass

Consistent with our reporter mouse analysis, only a subset of cells within the early pancreatic epithelium of the *Ptf1a-Cre; β-cat^{active}* mice exhibit evidence of β-catenin activation (Supplemental figure 1C). At birth, the gross pancreatic morphology of *Ptf1a-Cre; β-cat^{active}* appears similar to control (data not shown). Pancreatic mass is also equivalent at this time point (Fig. 2F, graph inset), suggesting that activation of β-catenin within the small number of cells of the early pancreatic epithelium in the *Ptf1a-Cre; β-cat^{active}* compared to the widespread activation in the *Pdx-Cre^{early}; β-cat^{active}* [28] is not sufficient to disrupt pancreas formation (Supplemental figure 1 B,C).

At P0, prominent ductal associated lesions are visible throughout the pancreas of the *Ptf1a-Cre; β-cat^{active}* mice (Fig. 2B). These lesions are not seen in control mice (Fig. 2A) or in *Pdx-Cre^{late}; β-cat^{active}*, which do not have any Cre activity in pancreatic ducts [28]. High levels of

nuclear-localized β-catenin are seen within these ductal associated lesions (Fig. 2D), while β-catenin is found exclusively at the plasma membrane in control animals (Fig. 2C). Despite their proximity to ductal structures, cells within the lesion that have elevated levels of β-catenin do not express the ductal marker, mucin 1 (Fig. 2D). Formal proof of the ductal origin of these cells is not possible without cell lineage tracing experiments. However, the location of these cells suggests a ductal source, indicating that activation of β-catenin may have caused some loss of differentiation in this population.

While pancreas morphology and mass is normal at P0, one month old *Ptf1a-Cre; β-cat^{active}* exhibit a grossly enlarged pancreas that is four times greater in mass than control (Fig. 2E). Pancreas mass continues to increase with age in the *Ptf1a-Cre; β-cat^{active}* (Fig. 2F), similar to what we have previously seen in *Pdx-Cre^{late}; β-cat^{active}* mice.

Ptf1aCre βcat^{active} develop large pancreatic tumors at a high frequency

Pancreatic tumors are not observed in *Pdx-Cre^{late}; β-cat^{active}* mice despite the dramatic increase in pancreatic mass [28]. However, large, well encapsulated tumors are detectable at the gross morphological level in *Ptf1a-Cre; β-cat^{active}* mice by three months of age (Fig. 3A). These tumors are slow-growing and non-metastatic; moreover, affected animals continue to eat and groom normally. By 12 months, nearly half of all mice exhibit large tumors, which are most often found in the ventral pancreas (Fig. 3B).

In cross section at the gross and histological levels, areas of necrosis (Fig. 3C, yellow), cystic structures (Fig. 3C,E *), and solid, pseudopapillary regions (Fig. 3C,E#) are visible. Some pancreas tissue, including acinar and islet structures, remains attached to the outer capsule of the tumor (Fig. 3E, arrows).

Although E-cadherin expression and membrane localization in the *Ptf1a-Cre; β-cat^{active}* pancreas is equivalent to control (Supplemental Figure 2A,B; Supplemental Figure 3A), its expression is downregulated within the tumors seen in those mice (Supplemental Figure 2C;Supplemental Figure 3A). The Wnt target genes, Axin2, cyclin D1, and p21 are significantly upregulated in the pancreata of *Ptf1a-Cre; β-cat^{active}* mice when compared to control (Fig. 3D, F, Supplemental Figure 3D), indicating that stabilization of β-catenin has resulted in robust activation of the canonical Wnt signaling pathway. Tumors isolated from *Ptf1a-Cre; β-cat^{active}* demonstrated an even greater increase in both Axin2 and cyclin D1 expression (Fig. 3D,F), as well as significant upregulation of p21, Cdk4, and c-jun expression (Supplemental Figure 3B,C,D), suggesting that further deregulation of the canonical Wnt pathway may be occurring during tumorigenesis.

Tumors in Ptf1aCre β-cat^{active} mice are morphologically similar to human SPN of the pancreas

Based upon published reports, upregulation of β-catenin is often seen in human SPN of the pancreas [16, 17]. Moreover, activating mutations within the third exon of the human β-catenin gene are also found in the majority of SPN's [18]. Therefore, we directly compared the morphology of a collection of human SPN tissue and the tumors observed in *Ptf1a-Cre; β-cat^{active}* mice.

We found that the mouse tumors recapitulated microscopic features that characterize SPNs in humans. Like the human tumors, all of the mouse tumors were well circumscribed with a distinct fibrous capsule (Fig. 4A,B, black arrows). Moreover, they exhibited extensive necrosis (Fig. 4C,D red arrow) and haemorrhage (Fig. 4C,D black arrows) centrally with preserved tissue typically being found at the periphery (Fig. 4A,B). The tumor cells in the subcapsular region were arranged in solid sheets and the intervening spaces were filled with haemorrhage

or necrotic debris. No glandular spaces were present. Focal calcifications were observed in one mouse tumor (data not shown), a feature that is sometimes seen in human SPN (Fig. 4C, green arrow). As in human SPN's (Fig. 4E,F) the mouse tumor cells were small, polygonal and monomorphic with a moderate amount of clear or pale eosinophilic cytoplasm. In addition, the mouse tumor cell nuclei were round to ovoid with dispersed, finely granular chromatin and inconspicuous nucleoli, features that are very similar to those seen in human SPN (Fig. 4E,F). Mitotic figures were rare in both human and mouse tumors.

In contrast to human cases of SPN, no eosinophilic hyaline globules or cholesterol clefts were identified in the mouse tumors, although foamy macrophages were often present. Nuclear grooves that are seen in human SPN's were also absent in the mouse tumors. A summary of our comparison of tumor morphology is presented in Supplemental Table 1.

Tumors in Ptf1aCre; β-cat^{active} mice have marker expression that is similar to human SPN

In order to characterize the molecular similarities between our cohort of human SPN tissue and the tumors present within the *Ptf1a-Cre; β-cat^{active}* mice, we analyzed the expression of a variety of well-established markers of SPN by immunohistochemistry. The human SPN samples in our collection demonstrated marker expression that is consistent with the published literature. The majority of human SPN's in our panel (11/13) had clear and dramatic upregulation of β-catenin, including strong cytoplasmic and nuclear localization (Fig. 5A). In comparison, β-catenin is exclusively localized to the plasma membrane in normal human pancreatic tissue (Fig. 5A). As expected, all tumors present in the *Ptf1a-Cre; β-cat^{active}* have similarly high levels of cytoplasmic and nuclear β-catenin (Fig. 5A). In support of the increased expression levels of Wnt target genes (Fig. 3, Supplemental Fig. 3), β-catenin is more robustly expressed in tumor tissue, than in the pancreas from *Ptf1a-Cre; β-cat^{active}* mice, where it remains preferentially partitioned to the nucleus (Fig. 5A).

All 13 human SPN samples expressed alpha-1 anti-trypsin and cyclin D1, while normal human pancreatic tissue is largely negative for both markers (Fig. 5B, C respectively). All tumors analyzed from *Ptf1a-Cre; β-cat^{active}* mice (6/6) also showed staining for alpha-1 anti-trypsin and cyclin D1 that was similar to the human SPN samples (Fig. 5B,C respectively). While the pancreas of *Ptf1a-Cre; β-cat^{active}* was negative for alpha-1 anti-trypsin (Fig. 5B) as in the human samples, cyclinD1 staining could be detected within exocrine cells (Fig. 5C). This increase is predicted by the quantitative PCR analysis shown previously (Fig 3F). Because cyclinD1 is a critical regulator of cell cycle progression, its upregulation in *Ptf1a-Cre; β-cat^{active}* may be partially responsible for the increase in pancreas mass observed (Fig. 2E).

All human and murine tumors tested were also positive for neuron specific enolase (NSE) (data not shown), while negative for chromogranin, AE1/AE3, clusterin, or estrogen receptor α, (data not shown). Neither the majority of human tumors (12/13) nor the murine tumors (6/6) expressed synaptophysin, a marker of endocrine differentiation (Fig. 5D). Murine tumors also did not express chymotrypsin, a marker of pancreatic exocrine cells (data not shown). The results of this marker comparison are summarized in Supplemental Table 2. These data demonstrate that the tumors found in *Ptf1a-Cre; β-cat^{active}* mice closely resemble human SPN at the immunohistochemical level.

PanIN formation is blocked in Ptf1a Cre β-cat^{active} Kras^{G12D} mice

Activating mutations in the GTP-ase Kras are found in over 90% of invasive pancreatic ductal adenocarcinomas (PDA) [29] and are thought to play a critical role in the formation of these highly lethal tumors [21, 30, 31]. A single amino acid change from glycine to aspartic acid, the most common site of mutation in human PDA, causes constitutive activation of Ras effector pathways. Previous reports using a mouse model in which expression of the *Kras^{G12D}*

oncogenic form is mediated by *Ptf1a-Cre*, have demonstrated that this mutation alone is sufficient to induce pancreatic intraepithelial neoplasia (PanIN), the most common precursor lesion to PDA [21, 32, 33]. Therefore, we asked whether aberrant activation of Kras in *Ptf1a-Cre; β-cat^{active}* mice might convert the SPN-like lesions into a more malignant tumor.

At 3 months of age, *Ptf1a-Cre; β-cat^{active}, Kras^{G12D}* mice have pancreata that are reduced in size compared to control and *Ptf1a-Cre; Kras^{G12D}* littermates (Fig. 6A). This loss of pancreatic mass in the *Ptf1a-Cre; β-cat^{active}, Kras^{G12D}* is striking given that *Ptf1a-Cre; β-cat^{active}* mouse littermates exhibit pancreatic hyperplasia (Fig. 6A) similar to what was previously described (Fig. 2E).

Histological analysis of the pancreas sections from *Ptf1a-Cre; β-cat^{active}, Kras^{G12D}* mice by hematoxylin/eosin staining reveals a dramatic loss of acinar cells replaced by small dilated ducts, suggestive of acinar to ductal metaplasia (Fig. 6B, Supplemental Fig. 4D). Moreover, the *Ptf1a-Cre; β-cat^{active}, Kras^{G12D}* mouse pancreas exhibits a substantial desmoplastic reaction that is more extensive than what is observed in the *Ptf1a-Cre; Kras^{G12D}* (confirmed by Gomori trichrome staining, data not shown). These mice also exhibit tumors with two distinct morphological patterns: cribriform and ductal (Fig. 6B; yellow * region with cribriform morphology; yellow # region with ductal morphology. Higher magnification pictures are shown in Supplemental Fig. 4D and E, F respectively). Lesions with similar morphology are not seen in the pancreas or in the SPN-like tumors of *Ptf1a-Cre; β-cat^{active}* mice (Fig. 6B; Fig. 4F; Sup Fig 4B), *Ptf1a-Cre; Kras^{G12D}* (Fig. 6B; Supplemental Fig. 4C) or in control littermates (Fig 6B; Supplemental Fig. 4A). Interestingly, few PanIN lesions consisting of ducts lined with mucinous columnar epithelium that are encountered with high frequency throughout the pancreas of *Ptf1a-Cre; Kras^{G12D}* (Fig. 6B, Supplemental fig. 4C) are found in *Ptf1a-Cre; β-cat^{active}; Kras^{G12D}* mice.

In order to confirm the relative absence of PanIN lesions in *Ptf1a-Cre; β-cat^{active}; Kras^{G12D}* mice, pancreas sections were stained with alcian blue which binds the acidic mucins produced by most PanINs. Cells with abundant alcian blue staining are frequently detected within pancreatic ducts exhibiting PanIN morphology in the *Ptf1a-Cre; Kras^{G12D}* mouse (Fig. 6C). However, alcian blue^{+} cells are not present in the *Ptf1a-Cre; β-cat^{active}; Kras^{G12D}* mouse (Fig. 6C, characteristic ductal lesions marked by #). Control and *Ptf1a-Cre; β-cat^{active}* (Fig. 6C) pancreatic tissue was also negative for alcian blue. Similar results were obtained with periodic acid/Schiff's reagent staining (PAS), which is known to mark PanINs (data not shown), indicating that PanIN formation is blocked in *Ptf1a-Cre; β-cat^{active} Kras^{G12D}* mice.

Lesions with ductal morphology in *Ptf1a-Cre; β-cat^{active}; Kras^{G12D}* mice contained cells whose cytoplasm was intensely stained for the ductal marker cytokeratin (CK) 19 (Fig. 6D, #), confirming that they have some degree of ductal differentiation. The areas of cribriform growth pattern in *Ptf1a-Cre; β-cat^{active}; Kras^{G12D}* mice were negative for CK19 (Fig. 6D, *). Pancreatic ducts within the *Ptf1a-Cre; β-cat^{active}* pancreas exhibit strong apical staining for CK19 that is equivalent to what is observed in control animals (Fig. 6D). PanIN lesions in *Ptf1a-Cre; Kras^{G12D}* mice were also strongly CK19 positive, which is consistent with previous reports[34] (Fig. 6D).

In order to determine whether the tumors in the *Ptf1a-Cre; β-cat^{active}; Kras^{G12D}* mice exhibit endocrine differentiation, pancreatic sections were stained with the islet marker synaptophysin. As expected, synaptophysin staining was localized exclusively to endocrine islets in control and *Ptf1a-Cre; β-cat^{active}* pancreatic tissue sections (Fig. 6E). However, in addition to synaptophysin^{+} islet structures, some scattered synpatophysin^{+}cells were found near PanIN lesions in *Ptf1a-Cre; Kras^{G12D}* samples (Fig. 6E). Both the cribriform and ductal lesions were negative for synaptophysin in *Ptf1a-Cre; β-cat^{active}; Kras^{G12D}* samples, suggesting a lack of

endocrine differentiation (Fig. 6E; *, cribriform; #, ductal; brown staining within the center of some cysts is background staining caused by the presence of cellular debris).

Tumors in *Ptf1a-Cre; β-cat^{active}, Kras^{G12D}* with cribriform morphology superficially resemble human acinar cell carcinoma, another rare, but aggressive, pancreatic neoplasm. Some cells within these lesions are arranged back-to-back with small lumens. The nuclei in these columnar cells are round to oval and basally located, with a moderate amount of eosinophilic cytoplasm (Fig. 6B,*; higher magnifications shown in Supplemental Fig. 2E,F). However, the cells are negative for markers of acinar differentiation, including amylase and chymotrypsin (data not shown). Moreover, they do not appear to have granules within the cytoplasm or the distinctively prominent nucleoli that are common hallmarks of human acinar cell carcinoma. Alternatively, these tumors display similarities to human intraductal tubular tumors[35–37]. Given the rare appearance of these tumors, the presence and level of Wnt signaling has not been investigated.

Together, the histological analysis of this cohort of mice demonstrates that activation of β-catenin in this particular context blocks the formation of lesions that are usually induced by Kras activation. Instead, tumor progression appears to have been shifted towards a different fate in *Ptf1a-Cre; β-cat^{active}; Kras^{G12D}* mice.

Hh responsive target gene expression is decreased in Ptf1aCre β-cat^{active} Kras^{G12D} murine lesions

In order to determine how Kras activation affects β-catenin protein level and localization, immunohistochemistry was performed on a cohort of mouse pancreas samples at three months of age. The cellular concentration of β-catenin is significantly higher in *Ptf1a-Cre; β-cat^{active}, Kras^{G12D}* tumors than it is in the *Ptf1a-Cre; βcat^{active}* pancreas (Fig. 7A). Moreover, β-catenin localization in *Ptf1a-Cre; β-cat^{active}; Kras^{G12D}* is strongly cytoplasmic and nuclear, while it remained exclusively nuclear and membrane bound in the *Ptf1a-Cre; βcat^{active}*. The further increase in β-catenin that occurred upon tumorigenesis in this model of Kras activation is similar to what was observed in the SPN-like tumors present in *Ptf1a-Cre; β-cat^{active}* mice (Fig. 5A). β-catenin concentration and plasma membrane localization in the *Ptf1a-Cre; Kras^{G12D}* pancreas appeared equivalent to control (Fig. 7A).

Quantitative analysis of Wnt target gene expression yielded results predicted by the level of pancreatic β-catenin in the different mouse samples. Upregulation of Axin2, Tcf1, p21, and CyclinD1 expression was measured in *Ptf1a-Cre; βcat^{active}* mice, with an even more robust increase occurring in *Ptf1a-Cre; β-cat^{active}; Kras^{G12D}* mice (Fig. 7D, Supplemental Fig. 5A, B, and data not shown, respectively). Axin2 and p21 expression levels in *Ptf1a-Cre; Kras^{G12D}* mice were equivalent to control (Fig. 7D, Supplemental Fig. 5B, respectively) while Tcf1 and cyclinD1 levels were slightly elevated (Supplemental Fig. 5 A, and data not shown, respectively). Interestingly, elevation of c-Myc was only seen in *Ptf1a-Cre; βcat^{active}*, while *Ptf1a-Cre; β-cat^{active}* and *Ptf1a-Cre; β-cat^{active}; Kras^{G12D}* remained equivalent to control (Supplemental Fig. 5C).

Previous reports have shown that pancreatic activation of Kras results in upregulation of the Hh and Notch signaling pathways [34, 3832]. Furthermore, this increased Hh and Notch pathway activity has been implicated in the formation of PanIN lesions and early PDA tumorigenesis [3940]. Therefore, we asked whether modulation of either of these pathways in *Ptf1a-Cre; β-cat^{active}, Kras^{G12D}* mice could account for the absence of PanIN formation. The majority of cells within both the cribriform and ductal lesions of the *Ptf1a-Cre; β-cat^{active}, Kras^{G12D}* are positive for the Notch target gene, Hes1 (Supplemental Fig 6D,E), which matches the frequency and intensity of the staining in the PanIN lesions in the *Ptf1a-Cre; Kras^{G12D}* (Supplemental Fig. 6C). Hes1 staining in the *Ptf1a-Cre; β-cat^{active}* is equivalent to control (Supplemental Fig.

6B,A respectively). This finding was confirmed by qPCR analysis of Hes1expression (Supplemental Fig. 5D).

Immunohistochemistry for Ptc, both a Hh receptor and transcriptional target of the signaling pathway, revealed strong staining within PanIN lesions in *Ptf1a-Cre; Kras^{G12D}* (Fig. 7B) mice. In contrast, no Ptc^{+} cells were detected in *Ptf1a-Cre; β-cat^{active}; Kras^{G12D}*, *Ptf1a-Cre; β-cat^{active}*, or control mice (Fig. 7B). Similar results were obtained for the Hh ligand, Sonic Hedgehog (Shh) (Fig. 7C). Quantitative PCR for Ptc and Gli1, another Hh pathway target gene, as well as for Shh and Indian Hh (Ihh) supports this result. While Ptc, Gli1, Shh, and Ihh expression is increased in *Ptf1a-Cre; Kras^{G12D}* pancreatic tissue, their expression remains equivalent to control in the *Ptf1a-Cre; β-cat^{active}; Kras^{G12D}* and *Ptf1a-Cre; β-cat^{active}* tissues (Supplemental Fig. 5E, F, Fig. 7E, F).

Previous reports have indicated that Kras activation can activate the MAPK and PI3 kinase pathways[38]. Therefore, we asked whether simultaneous activation of β-catenin and Kras in the *Ptf1a-Cre; β-cat^{active}; Kras^{G12D}* pancreas effected either MAPK or PI3 kinase activity. Western blotting of pancreatic lysates indicated that the level of MAPK phosphorylation in *Ptf1a-Cre; β-cat^{active}; Kras^{G12D}* was equivalent to that seen in *Ptf1a-Cre; Kras^{G12D}*; phosphorylated MAPK could not be detected in either control or *Ptf1a-Cre; β-cat^{active}* pancreatic tissue (Supplemental Fig. 7). However, an increase in Akt phosphorylation, a read-out of PI3 kinase activity, that is seen in *Ptf1a-Cre; Kras^{G12D}* (2 out of 3 animals) does not occur in *Ptf1a-Cre; β-cat^{active}, Kras^{G12D}* littermates (0 of 3 animals, Supplemental Fig. 7). Instead, pAKT levels in the *Ptf1a-Cre; β-cat^{active}, Kras^{G12D}* and *Ptf1a-Cre; β-cat^{active}* animals appear equivalent to control (Supplemental Fig. 7). Therefore, increased canonical Wnt signaling may block Kras dependent activation of PI3 kinase.

Thus, stabilization of β-catenin in the presence of an activating mutation in Kras results in a dramatic increase in canonical Wnt signaling and Notch signaling. Consequently, Kras activation no longer induces upregulation of the Hh signaling pathway and Akt phosphorylation. Further experimentation will be necessary to elucidate a mechanism to explain the molecular changes we have observed. However, it appears possible that these changes may partially explain the absence of PanIN lesions in *Ptf1a-Cre; β-cat^{active}, Kras^{G12D}* mice.

Discussion

Solid-pseudopapillary neoplasms are a rare human neoplasm that account for approximately 1% of pancreatic tumors [41]. Various groups have reported that over 90% of these tumors contain mutations that are predicted to interfere with the serine/threonine phosphorylation that is necessary to properly target β-catenin for degradation [18, 42]. Similar loss of this phosphorylation in *β-cat^{active}* mice, through Cre-mediated loss of the third exon, results in large tumors that appear closely related to human SPN. Thus, this study demonstrates for the first time that these human mutations in β-catenin are likely the proximate cause of SPN. Moreover, the *Ptf1a-Cre; β-cat^{active}* mouse is the first published murine model of this enigmatic tumor and proves that β-catenin stabilization, alone, is sufficient to induce SPN tumorigenesis within the appropriate cellular context. Interestingly, human SPNs most often occur in young females [41]. However, tumor frequency was equivalent in male and female mice and increased with age in the *Ptf1a-Cre; β-cat^{active}* mouse. This suggests that there might be different modifiers which alter human susceptibility to this pancreatic tumor.

Lineage tracing experiments are necessary to conclusively demonstrate that pancreatic ducts are the cells of origin in the SPN-like tumors we describe in the *Ptf1a-Cre; β-cat^{active}* mice. Unfortunately, efforts to create a mouse strain in which Cre-recombinase activity is restricted

to the pancreatic ductal compartment have been unsuccessful so far. However, comparing the phenotype we observe in the *Ptf1a-Cre; β-cat^{active}* with that of the *Pdx-Cre^{late}; β-cat^{active}* [28] provides compelling, although not definitive, evidence of a ductal origin for SPN. *Pdx-Cre^{late}* mice have Cre-recombinase activity in acinar cells and pancreatic islets, but not within pancreatic ducts. The pancreas of *Pdx-Cre^{late}; β-cat^{active}* mice grows to nearly 5 times the size of control littermates due to expansion of the exocrine compartment, a phenotype similar to that seen in *Ptf1a-Cre; β-cat^{active}* mice. In contrast, tumors did not develop in *Pdx-Cre^{late}; β-cat^{active}* mice or in another model of pancreatomegaly that is based on the conditional elimination of APC[43]. Conversely, *Ptf1a-Cre; β-cat^{active}* mice successfully activate β-catenin within pancreatic ducts, in addition to the islet and acinar compartments, resulting in a high frequency of SPN like tumors. While one cannot rule out the existence of a previously unappreciated cell population that is being selectively targeted by the *Ptf1a-Cre* and not the *PdxCre^{late}* mouse strain, it is likely that cells residing within the ductal compartment are responsible for the tumors observed. A schematic of the expression domains of the various mouse *Cre* strains we have used to stabilize β-catenin and their resultant phenotype is provided in Figure 8.

Our finding that concurrent activation of β-catenin in the *Kras^{G12D}* mouse diverts the cellular fate of neoplasms from PanIN's to novel ductal and cribriform tumor isoforms was particularly surprising. The *Ptf1a-Cre; Kras^{G12D}* mouse model has proven to be especially permissive to the formation of PDA in mice. The introduction of a variety of oncogenic mutations, such as the loss of the tumor suppressors p53 or Ink4a/Arf [44,34] into this model results in the formation of tumors with differing degrees of malignancy. More recently it has been shown that the introduction of other mutations in the *Ptf1a Cre; Kras^{G12D}* mouse model can shift the formation of PanIN lesions towards the formation of cystic neoplasms. The combination of a Kras mutation and Dpc4/Smad4 mutations in the mice results in the formation of mucinous cystic neoplasms (MCN) and intraductal papillary mucinous neoplasms (IPMN), respectively [45, 46]. These recently recognized entities are also thought to give rise to PDAC. In contrast to the Kras/DPC4 induced aberrations, the lesions we observed in Ptf1aCre; β-cat^{active}; Kras^{G12D} are not mucinous. Therefore, the activation of β-catenin in the context of a Kras activating mutation prevents the formation of PanIN lesions while resulting in other neoplastic alterations. The exact nature of these tumors remains to be established, but their ductal properties display similarities to recently defined intraductal tubular tumors (ITTs)[35–37], a subgroup of intraductal neoplasms possibly related to intraductal papillary-mucinous neoplasms (IPMN). However, because these ITTs have only recently been described, a direct comparison between *Ptf1a-Cre; β-cat^{active}; Kras^{G12D}* mouse and human tumors will need to be addressed in future studies. A discriminating feature of the tumors observed in the *Ptf1a-Cre; β-cat^{active}; Kras^{G12D}* mice is the absence of Hh signaling that is seen in PanIN lesions. It will be interesting to investigate the status of Hh signaling in human ITTs.

In conclusion, our study demonstrates that the context and sequence in which oncogenic mutations are acquired in the pancreas have a profound impact on tumor initiation and outcome. Moreover, our results suggest that the Wnt signaling pathway may act as a key determinant of tumor fate within the pancreas. Human pancreatic ductal adenocarcinoma is the 4th leading cause of cancer death in the United States. Current therapies are ineffective in treating this malignancy, resulting in a 5 year survival rate that is less than 5%. Our observation that stabilization of β-catenin dramatically alters the tumor phenotype in a mouse model of early PDA provides another window into the complex molecular circuitry involved in tumorigenesis. Further dissection of how β-catenin activation alters the downstream consequences of Kras activation might lead to novel therapeutic opportunities.

Supplementary Material

Refer to Web version on PubMed Central for supplementary material.

Abbreviations

PDA, pancreatic ductal adenocarcinoma; SPN, solid pseudopapillary neoplasms; PanIN, pancreatic intraepithelial neoplasia; Hh, Hedgehog.

Acknowledgments

We are indebted to Drs. Doug Melton, Chris Wright, Sunil Hingorani, and David Tuveson for providing the *Pdx-Cre*^{early}, *Ptf1a-Cre* mouse strains, and *Kras*^{G12D} respectively, and to Dr. Mike German for providing the Pdx1 antibody. We also thank Drs. Mike German and Gail Martin for helpful discussions, Jane Milliken for help with the human SPN immunohistochemistry, Micah Allen for histology support, Heather Heiser for the maintenance of our mouse stocks, and Don and Marcia Trask for imaging assistance. Work in M.H.'s laboratory was supported by grants from the NIH (CA112537) and the American Diabetes Association. P.W.H. was a part of the UCSF Biomedical Science graduate student program when this research was conducted. D.A.C. was supported by a postdoctoral fellowship from the California Institute of Regenerative Medicine (CIRM). Confocal and other images were generated in the UCSF Diabetes and Endocrinology Research Center microscopy core (P30 DK63720).

References

1. Gregorieff A, Clevers H. Wnt signaling in the intestinal epithelium: from endoderm to cancer. Genes Dev 2005;19:877–890. [PubMed: 15833914]
2. Fodde R, Brabletz T. Wnt/beta-catenin signaling in cancer stemness and malignant behavior. Curr Opin Cell Biol 2007;19:150–158. [PubMed: 17306971]
3. Polakis P. The many ways of Wnt in cancer. Current Opinion in Genetics & Development 2007;17:45–51. [PubMed: 17208432]
4. Reya T, Clevers H. Wnt signalling in stem cells and cancer. Nature 2005;434:843–850. [PubMed: 15829953]
5. Widelitz R. Wnt signaling through canonical and non-canonical pathways: recent progress. Growth Factors 2005;23:111–116. [PubMed: 16019432]
6. Murtaugh LC, Law AC, Dor Y, Melton DA. Beta-catenin is essential for pancreatic acinar but not islet development. Development 2005;132:4663–4674. [PubMed: 16192304]
7. Papadopoulou S, Edlund H. Attenuated Wnt signaling perturbs pancreatic growth but not pancreatic function. Diabetes 2005;54:2844–2851. [PubMed: 16186384]
8. Dessimoz J, Bonnard C, Huelsken J, Grapin-Botton A. Pancreas-specific deletion of beta-catenin reveals Wnt-dependent and Wnt-independent functions during development. Curr Biol 2005;15:1677–1683. [PubMed: 16169491]
9. Wells JM, Esni F, Boivin GP, Aronow BJ, Stuart W, Combs C, Sklenka A, Leach SD, Lowy AM. Wnt/beta-catenin signaling is required for development of the exocrine pancreas. BMC Dev Biol 2007;7:4. [PubMed: 17222338]
10. Heller RS, Dichmann DS, Jensen J, Miller C, Wong G, Madsen OD, Serup P. Expression patterns of Wnts, Frizzleds, sFRPs, and misexpression in transgenic mice suggesting a role for Wnts in pancreas and foregut pattern formation. Dev Dyn 2002;225:260–270. [PubMed: 12412008]
11. Koesters R, von Knebel Doeberitz M. The Wnt signaling pathway in solid childhood tumors. Cancer Lett 2003;198:123–138. [PubMed: 12957350]
12. Abraham SC, Wu TT, Hruban RH, Lee JH, Yeo CJ, Conlon K, Brennan M, Cameron JL, Klimstra DS. Genetic and immunohistochemical analysis of pancreatic acinar cell carcinoma: frequent allelic loss on chromosome 11p and alterations in the APC/beta-catenin pathway. Am J Pathol 2002;160:953–962. [PubMed: 11891193]
13. Al-Aynati MM, Radulovich N, Riddell RH, Tsao MS. Epithelial-cadherin and beta-catenin expression changes in pancreatic intraepithelial neoplasia. Clin Cancer Res 2004;10:1235–1240. [PubMed: 14977820]

14. Lowy AM, Fenoglio-Preiser C, Kim OJ, Kordich J, Gomez A, Knight J, James L, Groden J. Dysregulation of beta-catenin expression correlates with tumor differentiation in pancreatic duct adenocarcinoma. Ann Surg Oncol 2003;10:284–290. [PubMed: 12679314]
15. Zeng G, Germinaro M, Micsenyi A, Monga NK, Bell A, Sood A, Malhotra V, Sood N, Midda V, Monga DK, Kokkinakis DM, Monga SP. Aberrant Wnt/beta-catenin signaling in pancreatic adenocarcinoma. Neoplasia 2006;8:279–289. [PubMed: 16756720]
16. Nishimori I, Kohsaki T, Tochika N, Takeuchi T, Minakuchi T, Okabayashi T, Kobayashi M, Hanazaki K, Onishi S. Non-cystic solid-pseudopapillary tumor of the pancreas showing nuclear accumulation and activating gene mutation of beta-catenin. Pathol Int 2006;56:707–711. [PubMed: 17040296]
17. Min Kim S, Sun CD, Park KC, Kim HG, Lee WJ, Choi SH. Accumulation of beta-catenin protein, mutations in exon-3 of the beta-catenin gene and a loss of heterozygosity of 5q22 in solid pseudopapillary tumor of the pancreas. J Surg Oncol 2006;94:418–425. [PubMed: 16967453]
18. Abraham SC, Klimstra DS, Wilentz RE, Yeo CJ, Conlon K, Brennan M, Cameron JL, Wu TT, Hruban RH. Solid-pseudopapillary tumors of the pancreas are genetically distinct from pancreatic ductal adenocarcinomas and almost always harbor beta-catenin mutations. Am J Pathol 2002;160:1361–1369. [PubMed: 11943721]
19. Cao D, Maitra A, Saavedra JA, Klimstra DS, Adsay NV, Hruban RH. Expression of novel markers of pancreatic ductal adenocarcinoma in pancreatic nonductal neoplasms: additional evidence of different genetic pathways. Mod Pathol 2005;18:752–761. [PubMed: 15696124]
20. Harada N, Tamai Y, Ishikawa T, Sauer B, Takaku K, Oshima M, Taketo MM. Intestinal polyposis in mice with a dominant stable mutation of the beta-catenin gene. Embo J 1999;18:5931–5942. [PubMed: 10545105]
21. Hingorani SR, Petricoin EF, Maitra A, Rajapakse V, King C, Jacobetz MA, Ross S, Conrads TP, Veenstra TD, Hitt BA, Kawaguchi Y, Johann D, Liotta LA, Crawford HC, Putt ME, Jacks T, Wright CV, Hruban RH, Lowy AM, Tuveson DA. Preinvasive and invasive ductal pancreatic cancer and its early detection in the mouse. Cancer Cell 2003;4:437–450. [PubMed: 14706336]
22. Soriano P. Generalized lacZ expression with the ROSA26 Cre reporter strain. Nat Genet 1999;21:70–71. [PubMed: 9916792]
23. Lobe CG, Koop KE, Kreppner W, Lomeli H, Gertsenstein M, Nagy A. Z/AP, a double reporter for cre-mediated recombination. Dev Biol 1999;208:281–292. [PubMed: 10191045]
24. Kawaguchi Y, Cooper B, Gannon M, Ray M, MacDonald RJ, Wright CV. The role of the transcriptional regulator Ptf1a in converting intestinal to pancreatic progenitors. Nat Genet 2002;32:128–134. [PubMed: 12185368]
25. Gu G, Dubauskaite J, Melton DA. Direct evidence for the pancreatic lineage: NGN3+ cells are islet progenitors and are distinct from duct progenitors. Development 2002;129:2447–2457. [PubMed: 11973276]
26. Kawahira H, Ma NH, Tzanakakis ES, McMahon AP, Chuang PT, Hebrok M. Combined activities of hedgehog signaling inhibitors regulate pancreas development. Development 2003;130:4871–4879. [PubMed: 12917290]
27. Kim SK, Hebrok M, Melton DA. Notochord to endoderm signaling is required for pancreas development. Development 1997b;124:4243–4252. [PubMed: 9334273]
28. Heiser PW, Lau J, Taketo MM, Herrera PL, Hebrok M. Stabilization of beta-catenin impacts pancreas growth. Development 2006;133:2023–2032. [PubMed: 16611688]
29. Jaffee EM, Hruban RH, Canto M, Kern SE. Focus on pancreas cancer. Cancer Cell 2002;2:25–28. [PubMed: 12150822]
30. Tuveson DA, Hingorani SR. Ductal pancreatic cancer in humans and mice. Cold Spring Harb Symp Quant Biol 2005;70:65–72. [PubMed: 16869739]
31. Hezel AF, Kimmelman AC, Stanger BZ, Bardeesy N, Depinho RA. Genetics and biology of pancreatic ductal adenocarcinoma. Genes Dev 2006;20:1218–1249. [PubMed: 16702400]
32. Zhu L, Shi G, Schmidt CM, Hruban RH, Konieczny SF. Acinar cells contribute to the molecular heterogeneity of pancreatic intraepithelial neoplasia. Am J Pathol 2007;171:263–273. [PubMed: 17591971]

33. Aguirre AJ, Bardeesy N, Sinha M, Lopez L, Tuveson DA, Horner J, Redston MS, DePinho RA. Activated Kras and Ink4a/Arf deficiency cooperate to produce metastatic pancreatic ductal adenocarcinoma. Genes Dev 2003;17:3112–3126. [PubMed: 14681207]
34. Hingorani SR, Wang L, Multani AS, Combs C, Deramaudt TB, Hruban RH, Rustgi AK, Chang S, Tuveson DA. Trp53R172H and KrasG12D cooperate to promote chromosomal instability and widely metastatic pancreatic ductal adenocarcinoma in mice. Cancer Cell 2005;7:469–483. [PubMed: 15894267]
35. Tajiri T, Tate G, Inagaki T, Kunimura T, Inoue K, Mitsuya T, Yoshiba M, Morohoshi T. Intraductal tubular neoplasms of the pancreas: histogenesis and differentiation. Pancreas 2005;30:115–121. [PubMed: 15714133]
36. Albores-Saavedra J, Sheahan K, O'Riain C, Shukla D. Intraductal tubular adenoma, pyloric type, of the pancreas: additional observations on a new type of pancreatic neoplasm. Am J Surg Pathol 2004;28:233–238. [PubMed: 15043313]
37. Tajiri T, Tate G, Kunimura T, Inoue K, Mitsuya T, Yoshiba M, Morohosh T. Histologic and immunohistochemical comparison of intraductal tubular carcinoma, intraductal papillary-mucinous carcinoma, and ductal adenocarcinoma of the pancreas. Pancreas 2004;29:116–122. [PubMed: 15257103]
38. Pasca di Magliano M, Sekine S, Ermilov A, Ferris J, Dlugosz AA, Hebrok M. Hedgehog/Ras interactions regulate early stages of pancreatic cancer. Genes Dev 2006;20:3161–3173. [PubMed: 17114586]
39. Thayer SP, di Magliano MP, Heiser PW, Nielsen CM, Roberts DJ, Lauwers GY, Qi YP, Gysin S, Fernandez-del Castillo C, Yajnik V, Antoniu B, McMahon M, Warshaw AL, Hebrok M. Hedgehog is an early and late mediator of pancreatic cancer tumorigenesis. Nature 2003;425:851–856. [PubMed: 14520413]
40. Miyamoto Y, Maitra A, Ghosh B, Zechner U, Argani P, Iacobuzio-Donahue CA, Sriuranpong V, Iso T, Meszoely IM, Wolfe MS, Hruban RH, Ball DW, Schmid RM, Leach SD. Notch mediates TGF alpha-induced changes in epithelial differentiation during pancreatic tumorigenesis. Cancer Cell 2003;3:565–576. [PubMed: 12842085]
41. Klimstra DS, Wenig BM, Heffess CS. Solid-pseudopapillary tumor of the pancreas: a typically cystic carcinoma of low malignant potential. Semin Diagn Pathol 2000;17:66–80. [PubMed: 10721808]
42. Tanaka Y, Kato K, Notohara K, Hojo H, Ijiri R, Miyake T, Nagahara N, Sasaki F, Kitagawa N, Nakatani Y, Kobayashi Y. Frequent beta-catenin mutation and cytoplasmic/nuclear accumulation in pancreatic solid-pseudopapillary neoplasm. Cancer Res 2001;61:8401–8404. [PubMed: 11731417]
43. Strom A, Bonal C, Ashery-Padan R, Hashimoto N, Campos ML, Trumpp A, Noda T, Kido Y, Real FX, Thorel F, Herrera PL. Unique mechanisms of growth regulation and tumor suppression upon Apc inactivation in the pancreas. Development 2007;134:2719–2725. [PubMed: 17596282]
44. Bardeesy N, Aguirre AJ, Chu GC, Cheng KH, Lopez LV, Hezel AF, Feng B, Brennan C, Weissleder R, Mahmood U, Hanahan D, Redston MS, Chin L, Depinho RA. Both p16(Ink4a) and the p19(Arf)-p53 pathway constrain progression of pancreatic adenocarcinoma in the mouse. Proc Natl Acad Sci U S A 2006;103:5947–5952. [PubMed: 16585505]
45. Bardeesy N, Cheng KH, Berger JH, Chu GC, Pahler J, Olson P, Hezel AF, Horner J, Lauwers GY, Hanahan D, DePinho RA. Smad4 is dispensable for normal pancreas development yet critical in progression and tumor biology of pancreas cancer. Genes Dev 2006;20:3130–3146. [PubMed: 17114584]
46. Izeradjene K, Combs C, Best M, Gopinathan A, Wagner A, Grady WM, Deng CX, Hruban RH, Adsay NV, Tuveson DA, Hingorani SR. Kras(G12D) and Smad4/Dpc4 haploinsufficiency cooperate to induce mucinous cystic neoplasms and invasive adenocarcinoma of the pancreas. Cancer Cell 2007;11:229–243. [PubMed: 17349581]

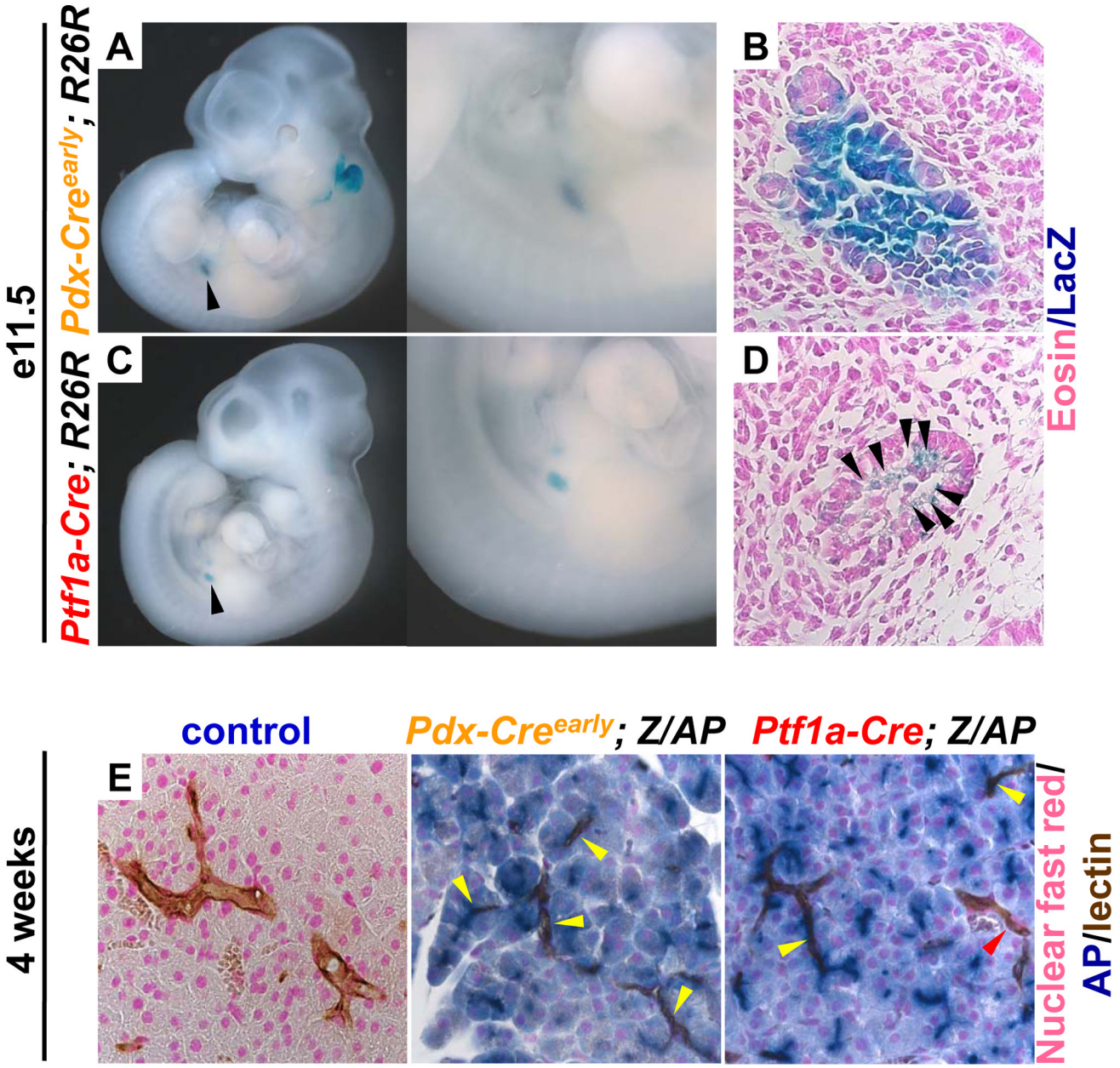

Figure 1. Ptf1a-Cre mice target a subset of early pancreatic progenitor cells and pancreatic ducts

Staining for *lacZ* marks cells that have undergone Cre mediated recombination in *Pdx-Cre*^{early} and *Ptf1a-Cre; R26R* mice. (A–D) e11.5 mouse embryos enzymatically stained for β-galactosidase activity. (A) *Pdx-Cre*^{early}*; R26R*, staining visible in the pancreas, indicated by black arrow, and enlarged. (C) *Ptf1a-Cre; R26R*, staining visible in the pancreas, indicated by a black arrow, and enlarged. (B,D) Histological examination of lacZ stained sections counterstained with eosin. (B) The majority of cells within the pancreatic epithelium of the *Pdx-Cre*^{early}*; R26R* are positive for β-galactosidase activity. (D) Equivalent section of a *Ptf1a-Cre; R26R* reveal that only a subset of cells within the pancreatic epithelium are positive for β-galactosidase activity (marked by black arrows). Staining for alkaline phosphatase (AP) marks cells that have undergone recombination in 4 week old *Pdx-Cre*^{early}*; Z/AP* and *Ptf1a-*

Cre; Z/AP mice. (E) Histological sections that have been enzymatically stained for alkaline phosphatase activity (blue), DBA lectin to mark pancreatic ducts (brown) and nuclear fast red as a counterstain (pink). No alkaline phosphatase activity is detectable in the control pancreas. The majority of acinar cells and most cells within pancreatic ducts (yellow arrows) exhibit clear alkaline phosphatase activity in the *Pdx-Cre^{early}; Z/AP* mouse. Almost all acinar cells and a subset of cells within pancreatic ducts (yellow arrows) have alkaline phosphatase activity in the *Ptf1a-Cre; Z/AP* mouse. Some pancreatic ducts do not contain cells that are positive for alkaline phosphatase (red arrow).

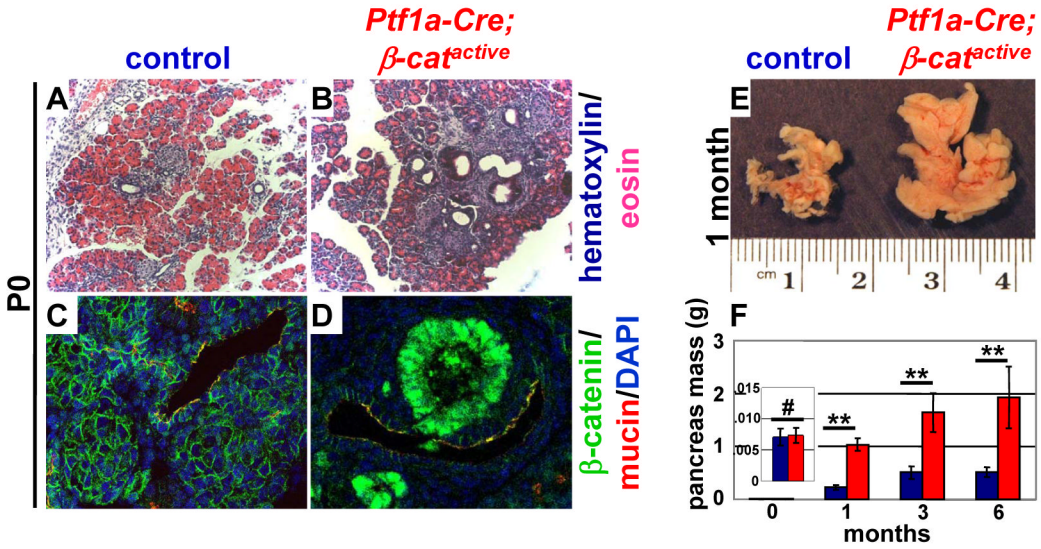

Figure 2. Activation of β-catenin in Ptf1a-Cre; β-cat^{active} mice causes ductal lesions and increased pancreas mass

Hematoxylin/eosin staining of pancreatic sections from P0 reveals the presence of prominent ductal lesions in the pancreata of *Ptf1a-Cre; β-cat^{active}* mice (B) that are not observed in the pancreata of control littermates (A). Strong nuclear accumulation of β-catenin (green) is seen in these ductal associated (duct labeled by mucin in red) lesions (D), while in control animals, β-catenin (green) remains localized to the plasma membrane in pancreatic ducts (C, ducts labeled by mucin in red). Cells that have nuclear localized β-catenin do not co-express mucin. Pancreata from *Ptf1a-Cre; β-cat^{active}* are significantly enlarged when compared to control at one month of age (E). Quantitative measurements revealed an approximately 4 fold increase in pancreatic mass at 6 months of age (F, n≥7 for each time point analyzed; control, blue; *Ptf1a-Cre; β-cat^{active}*, red). Confidence intervals were calculated using student's t-test. P values: #, not significant; **, p<0.01. Error bars represent standard error of the mean.

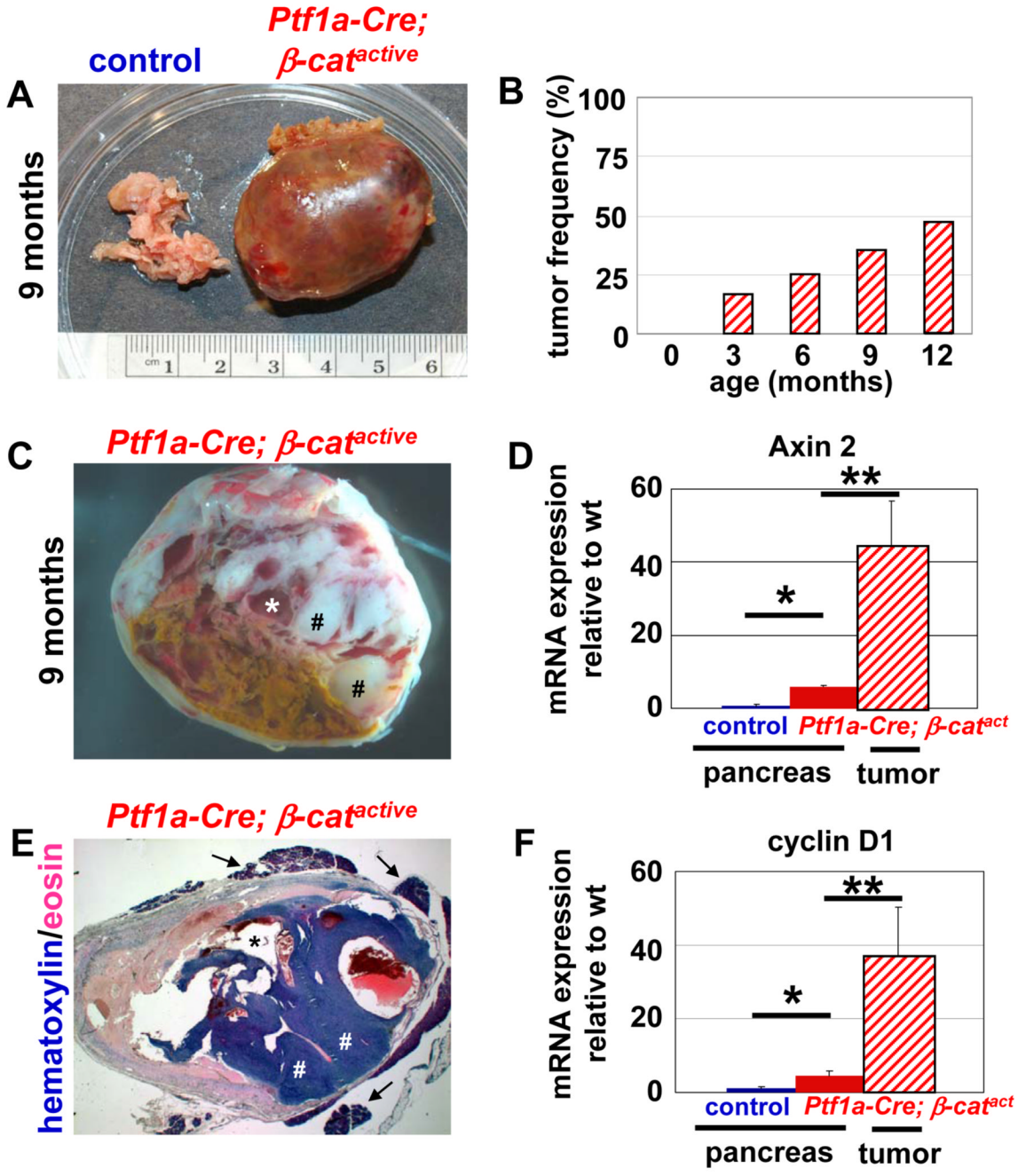

Figure 3. Ptf1a-Cre; βcat^{active} develop large pancreatic tumors at a high frequency

Gross morphology of a typical tumor seen in the pancreas of *Ptf1a-Cre; β-cat^{active}*, aged 9 months (A, right) compared to a pancreas from a littermate control (A, left). Gross morphology of a cross section of the murine tumor reveals pseudopapillary regions (C, labeled by #) and cystic structures (C, labeled by *). Histological examination of the murine tumor (x12 magnification) show the pseudopapillary regions (E, labeled by #), cystic structures (E, labeled by *) and the pancreatic remnant surrounding the tumor (E, labeled by arrow). Tumors are first detectable in *Ptf1a-Cre; β-cat^{active}* mice at 3 months of age. By 12 months of age, nearly 50% of *Ptf1a-Cre; β-cat^{active}* mice exhibit tumors (B; n≥8 for each time point examined). Expression of the Wnt target genes, Axin 2 (D) and cyclinD1 (F) are significantly upregulated in the *Ptf1a-*

Cre; β-cat^{active} pancreas when compared to control pancreas at 9 months of age by RT-PCR. Tumors found in *Ptf1a-Cre; β-cat*^{active} mice exhibit a further increase in overexpression of Axin 2 (D) and cyclinD1 (F). Confidence intervals were calculated using student's t-test, $n \geq 3$. P values: #, not significant; *, $p<0.05$; **, $p<0.01$. Error bars represent standard deviation.

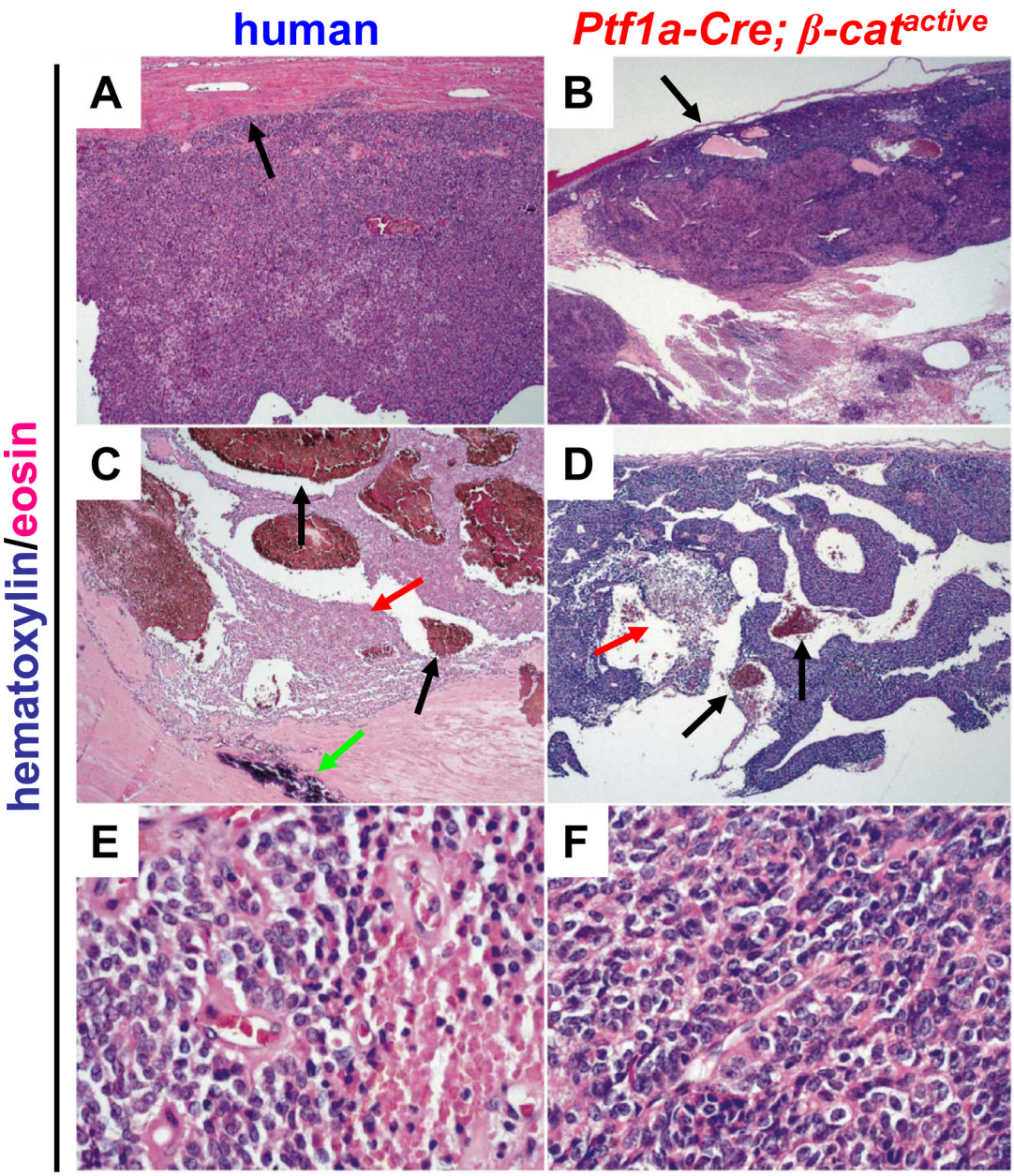

Figure 4. Tumors in Ptf1a-Cre; β-cat^{active} mice are morphologically similar to human solid pseudopapillary tumors of the pancreas

Slides were stained with hematoxylin and eosin to provide contrast. Low power view (x50) of human SPN (A) and murine tumor (B). Black arrows indicate tumor capsule (A,B). Low power view (x50) of human SPN (C) and murine tumor (D) with black arrows indicating areas of haemorrhage (C,D), red arrows indicating areas of necrosis (C,D), and green arrow to indicate a site of calcification (C). High power view (x400) of human SPN (E) and murine tumors (F). Images shown are representative samples from 13 human and 6 murine tumors analyzed; mice were 9 months old.

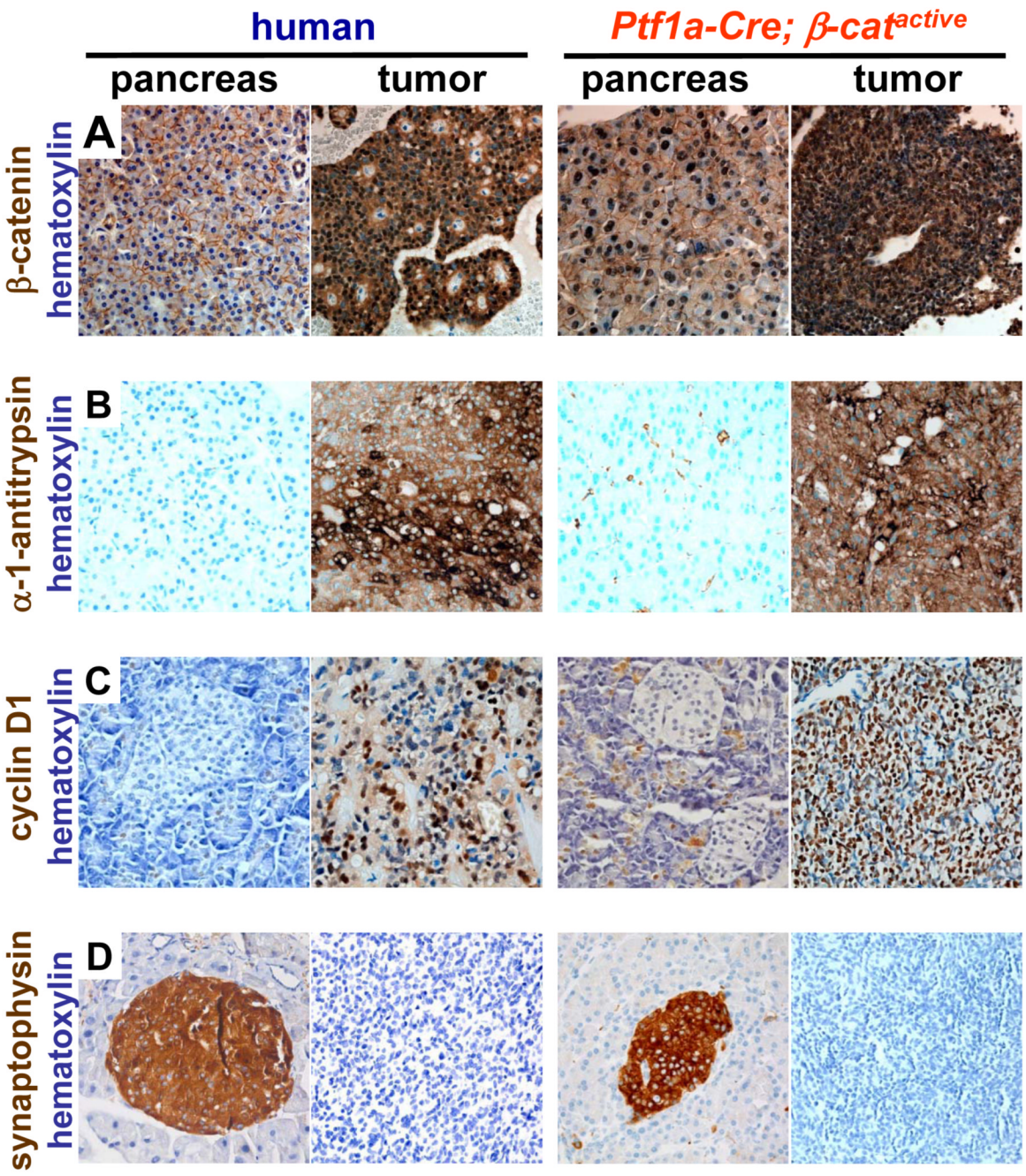

Figure 5. Tumors in Ptf1a-Cre; β-cat^{active} mice have marker expression that is similar to human SPN

(A) Normal human pancreas showing membranous β-catenin staining and pancreas from *Ptf1a-Cre; β-cat^{active}* mice exhibiting membranous and nuclear accumulation of β-catenin. Both human SPN's and the murine tumors show marked cytoplasmic and nuclear staining for β-catenin. (B) Alpha-1 anti-trypsin was expressed in human SPN and murine tumors with a globular pattern but was not expressed in normal human or *Ptf1a-Cre; β-cat^{active}* pancreas. (C) cyclinD1 was expressed at high levels in human SPN and murine tumors. Elevated levels of cyclinD1were also detected in the exocrine tissue of the *Ptf1a-Cre; β-cat^{active}* pancreas. Cyclin D1 was not detected in normal human pancreas tissue. (D) Neither human SPN's, nor murine

tumors, express synaptophysin. Synaptophysin is detectable in both normal human pancreatic islets and the islets of *Ptf1a-Cre; β-cat*^{active} mice. All images were acquired at high magnification (x400); tissues were counterstained with hematoxylin to improve contrast; mice were 9 months old.

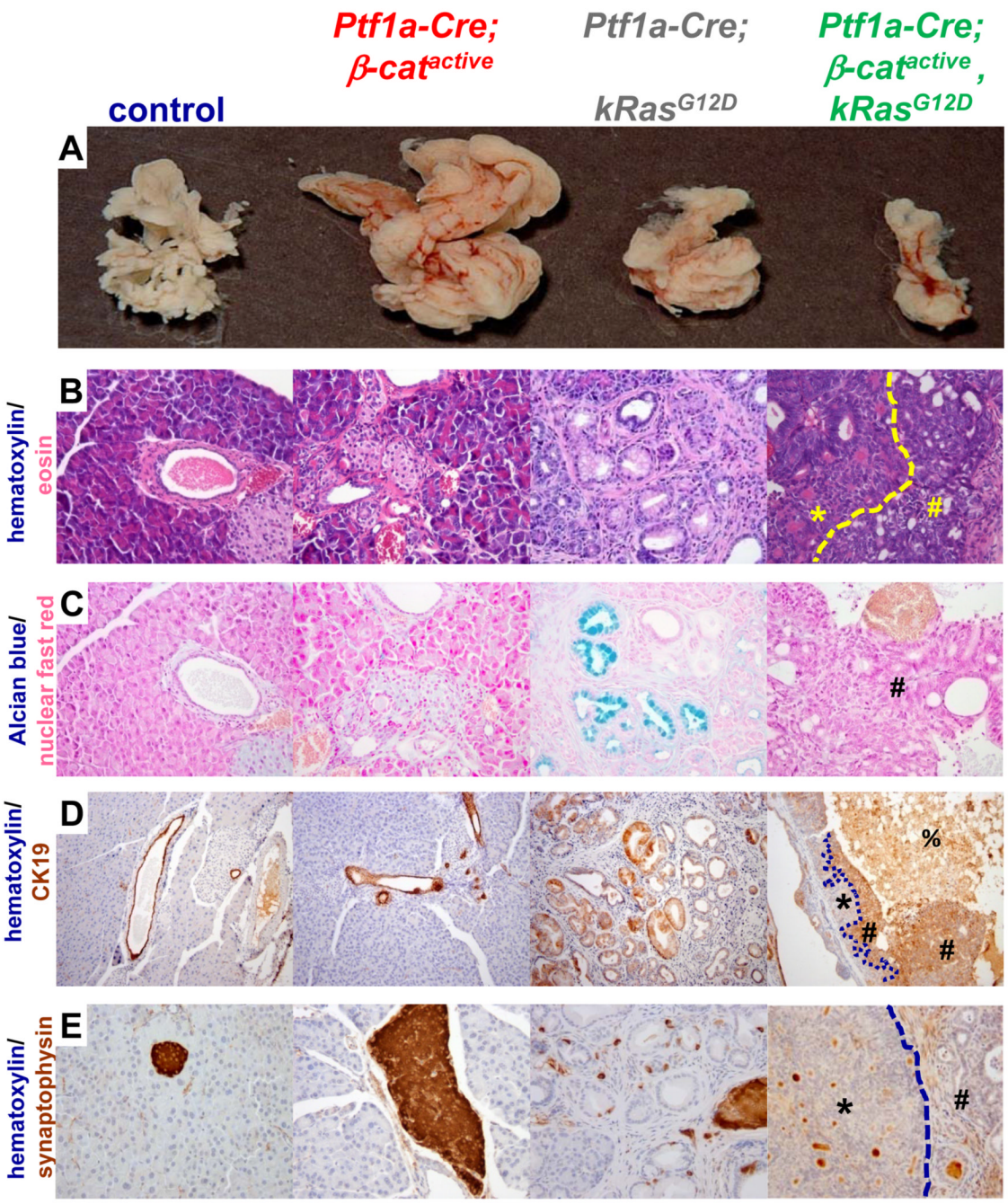

Figure 6. PanIN lesions do not form in Ptf1a-Cre; β-cat^{active}, Kras^{G12D} mice

(A–E) 3 month old pancreata. (A) Pancreas size is reduced and morphology is condensed in *Ptf1a-Cre; β-cat^{active}, Kras^{G12D}* mice when compared to control or *Ptf1a-Cre; Kras^{G12D}* organs. *Ptf1a-Cre; β-cat^{active}* mice exhibit pancreatic hyperplasia in this mouse background that is equivalent to what was previously described. (B) Hematoxylin (blue)/eosin (pink) pancreas sections, 400x magnification. Two distinct tumor types that frequently form within *Ptf1a-Cre; β-cat^{active}* mice have ductal- (B, yellow #) or cribriform (B, yellow *, separated by dashed yellow line) morphology. Lesions were found in all mice analyzed (n=5). Similar lesions are not found in control, *Ptf1a-Cre; β-cat^{active}*, or *Ptf1a-Cre; Kras^{G12D}* mice. The characteristic columnar cells found within ductal lesions in the *Ptf1a-Cre; Kras^{G12D}* are not

seen in the *Ptf1a-Cre; β-cat*^{active}*;Kras*^{G12D}. (C) alcian blue and nuclear fast red stained pancreas sections, 400x magnification. Alcian blue staining, a hallmark of PanIN that is apparent throughout the *Ptf1a-Cre;Kras*^{G12D} tissue, is not seen in *Ptf1a-Cre; β-cat*^{active}, *Kras*^{G12D} mice (# ductal lesion). Alcian blue was not detected in control or *Ptf1a-Cre; β-cat*^{active} tissue. (D) CK19 (brown) and hematoxylin (blue) stained pancreatic sections, 100x magnification. Normal ducts are marked by CK19 expression in control and *Ptf1a-Cre;β-cat*^{active} pancreatic tissue, as are the characteristic PanIN lesions in the *Ptf1a-Cre; Kras*^{G12D} pancreas. Cells with ductal morphology in the *Ptf1a-Cre; β-cat*^{active}, *Kras*^{G12D} (#) are positive for CK19. Cells with cribriform morphology do not express CK19 (*, boundary between distinct lesion types indicated by dashed line). Necrotic debris exhibits non-specific staining (%). (E) synaptophysin (brown) and hematoxylin (blue) stained pancreatic sections, 400x magnification. Pancreatic islets within control, *Ptf1a-Cre; βcat*^{active}, and *Ptf1a-Cre;Kras*^{G12D} are synaptophysin positive. Neither the ductal (#) nor the cribriform (*) lesions are synaptophysin^{+}. Brown staining visible in the *Ptf1a-Cre; β-cat*^{active}, *Kras*^{G12D} is non-specific staining of debris within cystic structures. Images are representative of n≥7 samples for each mouse genotype indicated; mice were 3 months old.

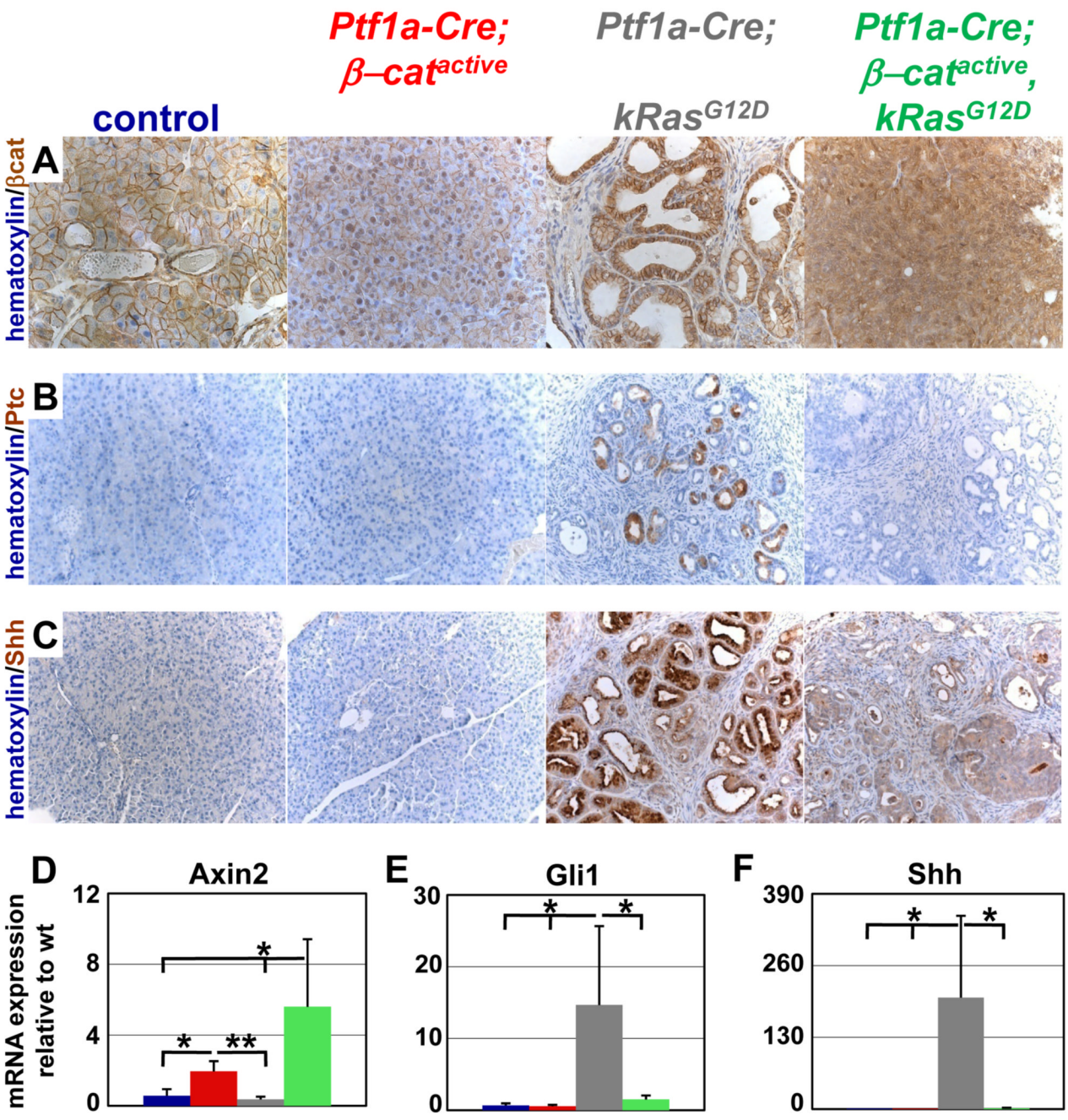

Figure 7. Hh responsive target gene expression is decreased in Ptf1aCre β-cat^{active} Kras^{G12D} murine lesions

(A) β-catenin (brown) and hematoxylin (blue) stained pancreatic sections. β-catenin is preferentially localized to the plasma membrane and nucleus within the pancreas of *Ptf1a-Cre; β-cat^{active}*. Lesions within the *Ptf1a-Cre; β-cat^{active}, Kras^{G12D}* mice exhibit even stronger nuclear staining for β-catenin, along with high levels of cytoplasmic staining. β-catenin remains localized only to the plasma membrane in control and *Ptf1a-Cre; Kras^{G12D}* pancreata. (B) Ptc (brown) and hematoxylin (blue) stained pancreatic sections. Cells within PanIN lesions in the *Ptf1a-Cre; Kras^{G12D}* show strong Ptc staining. Ptc staining in the *Ptf1a-Cre; β-cat^{active}, Kras^{G12D}* lesion is equivalent to the background staining seen in control and *Ptf1a-Cre; β-*

cat^{active} pancreata. (C) Shh (brown) and hematoxylin (blue) stained pancreatic sections. Robust staining for Shh ligand is seen in the majority of the remaining epithelial cells and PanIN lesions in the *Ptf1a-Cre; Kras*^{G12D} pancreas. Shh staining within the lesions in the *Ptf1a-Cre; β-cat*^{active}*, Kras*^{G12D} is only slightly higher than the background staining in control and *Ptf1a-Cre; β-cat*^{active} pancreata. (D–F) Graphs showing quantitative PCR normalized to wild type control; control (blue); *Ptf1a-Cre; β-cat*^{active} (red); *Ptf1a-Cre;Kras*^{G12D} (grey); *Ptf1a-Cre; β-cat*^{active}*, Kras*^{G12D} (green). Significant upregulation of the canonical Wnt target gene Axin2 was detected in *Ptf1a-Cre; β-cat*^{active} murine pancreatic tissue when compared to control and *Ptf1a-Cre; Kras*^{G12D} pancreas (D). Further upregulation of these target genes was measured in *Ptf1a-Cre; β-cat*^{active}*, Kras*^{G12D} pancreatic tissue when compared to the *Ptf1a-Cre; β-cat*^{active} (D). Significant upregulation of the Hh responsive target genes Gli was seen only in the *Ptf1a-Cre; Kras*^{G12D} (E). mRNA expression of Gli was equivalent in control, *Ptf1a-Cre; β-cat*^{active}, and *Ptf1a-Cre; β-cat*^{active}*, Kras*^{G12D} pancreatic tissue (E). Strong upregulation of the Hh ligand, Shh, was also detected exclusively in *Ptf1a-Cre; Kras*^{G12D} samples (F). No significant increase in the expression of this ligand was found in control, *Ptf1a-Cre; β-cat*^{active}, and *Ptf1a-Cre; β-cat*^{active}*, Kras*^{G12D} samples (F). All image data shown in this figure came from 3 month old mice. Images are representative of n≥7 samples for each mouse genotype indicated. Quantitative PCR was conducted on mRNA isolated from n=3 animals from each genotype. Error bars represent standard deviation. Confidence intervals were calculated using student's t-test. P values: #, not significant; *, $p<0.05$; **, $p<0.01$; mice were 3 months old.

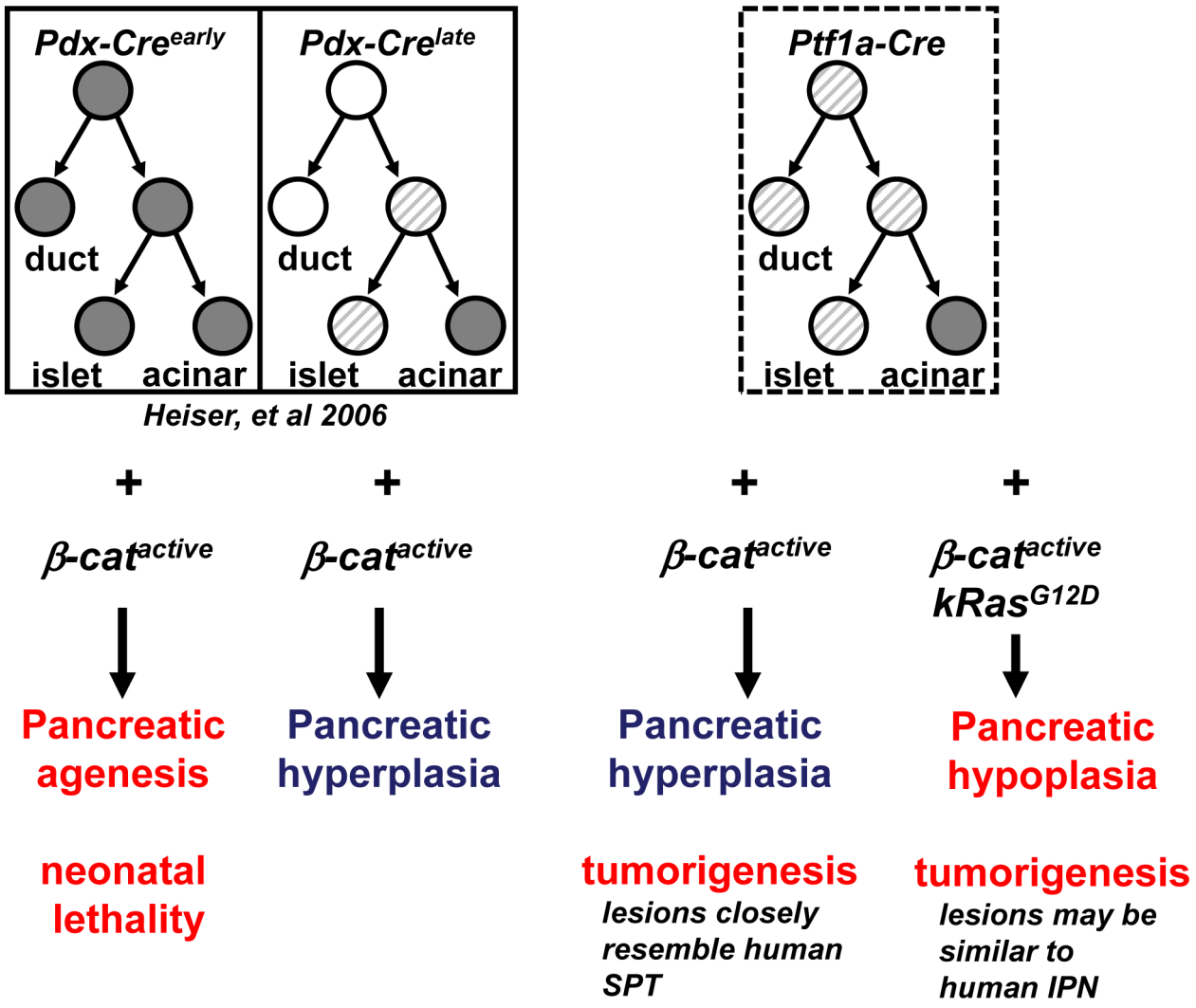

Figure 8. Comparison of Cre expression domains of Pdx-Cre^{early}, Pdx-Cre^{late}, and Ptf1a-Cre

Schematic illustrates the cellular compartments targeted by the different pancreatic mouse *Cre* strains, and their respective phenotype when crossed to the β-*cat^{active}* mouse. White circles indicate no Cre expression. Gray striped circles indicate mosaic Cre expression. Dark gray circles indicate robust Cre expression.